Application of the complex beam parameter to the design of a quasioptical transmission line for a submillimetre wave gyrotron

Application of the complex beam parameter to the design of a quasi-optical transmission line for a submillimetre wave gyrotron

I. OGAWA , A. SAKAI , T. IDEHARA and W. KASPAREK

The complex beam parameter can be used to facilitate the design of a quasi-optical transmission line which converts the output of a submillimetre wave gyrotron into a well collimated, linearly polarized beam. The quality of the beam produced by the quasi-optical antenna is improved further by removing any sidelobes. Only a small fraction of the beam power is sacrificed.

1. Introduction

Electromagnetic waves in the submillimetre wavelength range have applications in many fields including spectroscopy, the measurement of material properties and plasma diagnostics. Until recently, molecular vapour lasers have been the only power sources at these wavelengths (for example, Semet *et al.* (1980), Kawahata *et al.* (1988)). Like plasma scattering measurement and Thomson scattering, some applications need more intense waves (Fekete *et al.* 1994, Suvorov *et al.* 1997). High frequency gyrotrons have clear advantages at submillimetre wavelengths because of their capacity to deliver high powers (Hong *et al.* 1992, Idehara *et al.* 1992, 1993).

Before these gyrotrons can be used as power sources, it is necessary to convert the output into a well collimated, linearly polarized beam. Unlike molecular vapour lasers, gyrotrons produce hollow cone-shaped beams, which are far from what is usually required.

We have proposed the use of a quasi-optical transmission line to convert the output into a high quality beam (Ogawa *et al.* 1997). The system consists of a quasi-optical antenna and a series of mirrors, including an elliptical mirror for beam collimation. The quasi-optical antenna converts the gyrotron output into a linearly polarized beam. This beam has sidelobes which are truncated by setting the size of an elliptical mirror located far from the antenna. The resulting high-quality beam is obtained at the expense of some power loss. The loss is small enough to be acceptable in the low-power case, unlike high-power gyrotron applications.

In our design, the Huygens equation can be used to calculate the intensity profile of the beam produced at any point along its path.

However, if Gaussian optics can be applied, because of the long distance between the quasi-optical antenna and the elliptical mirror, the calculation time for the design of an optimized system can be significantly reduced. The main purpose of this paper is to demonstrate the effectiveness of this approach.

2. Spreading of beam produced by image source

2.1. Description of the image source

The first element in the transmission line is the quasi-optical antenna consisting of a circular waveguide with a step-cut and a parabolic reflector (see figure 1) (Vlasov and Orlova 1974). The quasi-optical antenna converts the gyrotron output into a linearly polarized beam with polarization in the x-direction. The beam produced has a rectangular cross-section (length D_H and width D_E) and propagates in the direction $(0, \cos \alpha, \sin \alpha)$, where α is the emission angle. These values are determined by the following equations

$$\alpha = \sin^{-1} \frac{\lambda \xi'_{mn}}{2\pi a_w} \tag{1}$$

$$D_E = 4f_p \tag{2}$$

$$D_H = 4a_w \cos \alpha \tag{3}$$

where f_p is the focal length of the parabolic cylinder, a_w the waveguide radius, ξ'_{mn} the nth root of $J'_m(\xi) = 0$, and λ the wavelength.

Radiation reflected from the parabolic reflector of the quasi-optical antenna is treated as if it comes from a plane image source lying behind the parabolic reflector with emission angle α. The fields over this image source for a TE_{0n} mode, calculated using geometrical optics (Wada and Nakajima 1986, Brand et al. 1990), are

$$E_x = \left(1 + \frac{x^2}{4f_p^2}\right)^{-1/2} \exp\left(-jky \cos \alpha\right)$$

$$E_y = 0$$

$$E_z = 0$$

$$X_x = 0 \tag{4}$$

$$H_y = \frac{E_x}{\eta} \sin \alpha$$

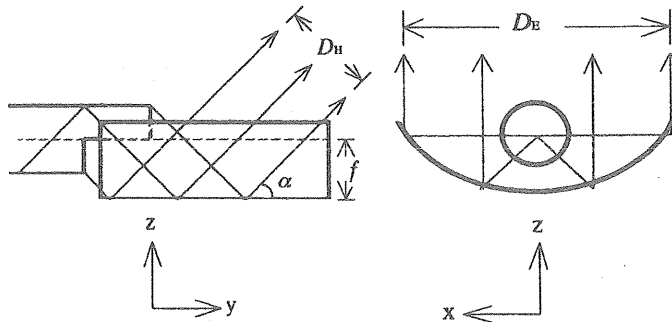$$H_z = -\frac{E_x}{\eta} \cos \alpha$$

Figure 1. Quasi-optical antenna.

in the region $-2f_p < x < 2f_p$, $-2a_w \cot \alpha < y < 2a_w \cot \alpha$, and zero elsewhere. η is the wave impedance. The origin $(0,0,0)$ is set at the centre of the image source. The fields for a TE_{1n} mode are obtained by multiplying E_x in (4) by $\cos\phi$ because it varies with $\cos\phi$, where ϕ is an azimuthal angle. It follows that, for this case, we can use equation (4) if we replace E_x by

$$E_x = \left(1 + \frac{x^2}{4f_p^2}\right)^{-3/2} \left(1 - \frac{x^2}{4f_p^2}\right) \exp\left(-jky\cos\alpha\right). \tag{5}$$

When the Poynting vector at the image source is calculated, it is easy to see that in both cases these fields describe a beam propagating in the direction $(0, \cos\alpha, \sin\alpha)$ with a rectangular cross-section.

2.2. Fields at a distance point

The intensity profiles of the beam are obtained by the boundary value problem of the Helmholtz equation for the image source. Its solution is equivalent to the calculation of the Huygens equation, which can be written as

$$\psi_P = \frac{jk}{4\pi} \int\int_A \psi_S \frac{\exp\left(-jkR\right)}{R} (\hat{r} + \hat{s}) \cdot \hat{n}\, ds \tag{6}$$

where A is the plane image source region, R the distance between a source point S on A and the field point P, $\hat{r}$ the unit vector from point S on A to P, $\hat{n}$ the normal vector to A and $\hat{s}$ the unit vector in the direction of the Poynting vector at the source point. If a field quantity ψ_S is given at all points on A, then ψ_P at any point can be obtained by using this equation. Thus we can obtain the electromagnetic fields at P by applying (6) to the three components of electric and magnetic fields.

2.3. Spreading of beams produced by image sources

In order to investigate how the beams spread, their intensity profiles have been calculated for a plane at a distance z from the image source. The image source given by (4) and (5) is now rotating around the x-axis by $(90° - \alpha)$ so that the beam produced propagates along the z-axis (figure 2). The intensity profiles for the TE_{15} mode ($f = 354\,GHz$, $f_p = 21.75\,mm$, $a_w = 14\,mm$) are shown in figure 3. Contours
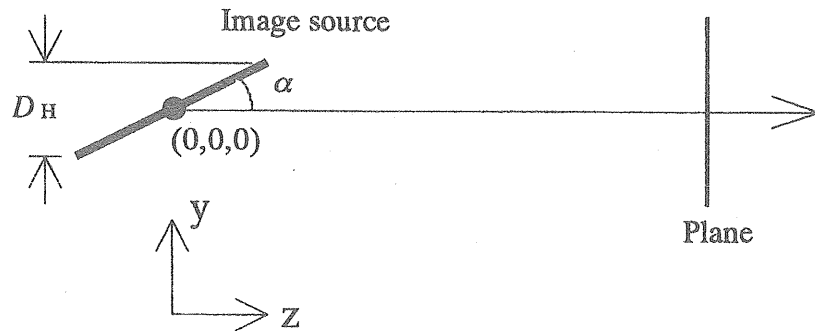

Figure 2. Plane image source used in the calculation of the subsequent radiation patterns of the quasi-optical antenna with a single parabolic reflector. The beam propagates along the z-axis.
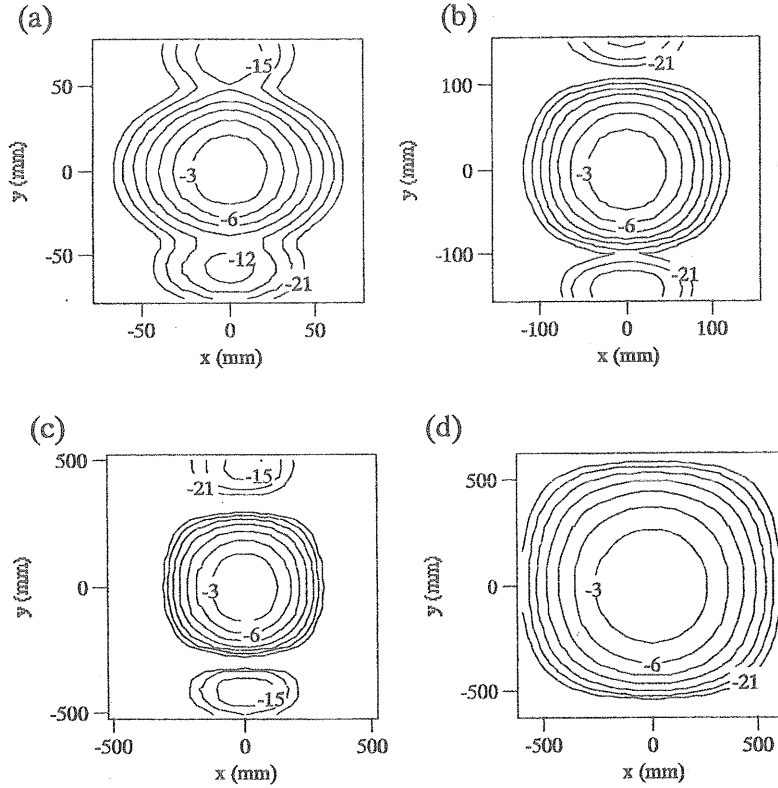
Figure 3. Calculated intensity contours at various distances z from the image source: (a) $z = 3000\,\text{mm}$; (b) $z = 7000\,\text{mm}$; (c) $z = 20\,000\,\text{mm}$; (d) $z = 40\,000\,\text{mm}$. Contours are in decibels relative to the intensity maximum.

are in decibels relative to the intensity maximum. For this mode, the emission angle α is 8.23° and the beam widths D_E and D_H and 87.0 mm and 55.4 mm respectively.

According to Gaussian optics, the beam intensity is given by

$$I = \frac{w_{0x}w_{0y}}{w_{Gx}w_{Gy}} \exp\left(-\frac{2x^2}{w_{Gx}^2}\right) \exp\left(-\frac{2y^2}{w_{Gy}^2}\right) \qquad (7)$$

where w_{0x} and w_{0y} are the beam waist sizes, and w_{Gx} and w_{Gy} are the spot sizes defined by

$$w_{Gx} = w_{0x}\left(1 + \frac{\lambda^2 z^2}{\pi^2 w_{0x}^4}\right)^{1/2} \qquad (8)$$

and

$$w_{Gy} = w_{0y}\left(1 + \frac{\lambda^2 z^2}{\pi^2 w_{0y}^4}\right)^{1/2} \qquad (9)$$

All of these sizes are the half-widths of the $-8.69\,\text{dB}$ (or e^{-2}) contours. Such a beam is described as bi-Gaussian. The beam spot sizes w_x and w_y are listed in table 1

z (mm)	3000	7000	20 000	40 000
w_x (mm)	38.9	75.9	214	426
$w_x/w_{Gx}(w_{0x} = 25.4\,\text{mm})$	0.95	0.97	1.0	1.0
w_y (mm)	33.4	74.9	214	429
w_y/w_{Gy} $(w_{0y} = 25.3\,\text{mm})$	0.82	0.95	1.0	1.0

Table 1. Spot sizes of the beam produced by the image source for the TE_{15} mode ($f = 354\,\text{GHz}$, $f_p = 21.75\,\text{mm}$, $a_w = 14\,\text{mm}$) as a function of distance z. w_{Gx} and w_{Gy} denote spot sizes of a Gaussian beam with waist sizes of w_{0x} and w_{0y}

as a function of distance z. The beam waist sizes calculated from the spot sizes at $z = 40\,000\,\text{mm}$ using (8) and (9) are $w_{0x} = 25.4\,\text{mm}$ and $w_{0y} = 25.3\,\text{mm}$, respectively. The ratios w_x/w_{Gx} and w_y/w_{Gy} demonstrate that the spot size for larger z are accurately given by Gaussian optics. This is expected to be the case in the far field where $z \gg z_F$, given by

$$z_F = \tfrac{1}{4}k(D_E^2 + D_H^2) \tag{10}$$

In the present case, the value of z_F is $19\,700\,\text{mm}$.

The waist sizes of the equivalent bi-Gaussian beam are obtained for image sources at various gyrotron operating wavelengths (table 2). The waist size w_{0y} depends mainly on the only length D_H and the waist size w_{0x} depends mainly on the only width D_E. The ratio w_{0y}/D_H is approximately equal to 0.46 and the ratio w_{0x}/D_E is approximately equal to 0.44 for TE_{0n} modes and 0.30 for TE_{1n} modes. These results can be used as the starting point for the design of a quasi-optical antenna which can produce a far field with circular cross-section. We will show this for the TE_{15} mode case where $D_E = 87.0\,\text{mm}$ and $D_H = 55.4\,\text{mm}$. We will treat the beam as Gaussian with a waist size of $w_0 = 25.4\,\text{mm}$ because its cross-section is almost circular ($w_{0x} = 25.4\,\text{mm}$, $w_{0y} = 25.3\,\text{mm}$), and use the complex beam parameter. This will lead to a method of designing systems that requires much less computation time.

Mode	f (GHz)	α (°)	z_F (mm)	D_E (mm)	w_{0x}/D_E	D_H (mm)	w_{0y}/D_H
TE_{03}	301	6.62	10 500	60.0	0.43	55.6	0.46
			16 800	87.0	0.44	55.6	0.45
			20 600	100.0	0.44	55.6	0.46
TE_{06}	388	9.93	13 500	60.0	0.43	55.2	0.46
			21 600	87.0	0.44	55.2	0.46
			26 500	100.0	0.44	55.2	0.46
TE_{15}	354	8.23	12 400	60.0	0.30	55.4	0.46
			19 700	87.0	0.29	55.4	0.46
			24 200	100.0	0.30	55.4	0.46
TE_{18}	718	9.30	13 100	44.0	0.29	39.5	0.46
			19 400	60.0	0.30	39.5	0.46
			34 300	87.0	0.30	39.5	0.46

Table 2. Waist sizes of equivalent bi-Gaussian beam obtained for various image sources. These sizes are compared with beam widths D_E and D_H.

3. Estimation of the position and size of beam waist by using the complex beam parameter

3.1. *Description of the complex beam parameter*

A Gaussian beam with waist size w_0 has a wave front with a radius of curvature given by

$$R = z \left(1 + \frac{\pi^2 w_0^4}{\lambda^2 z^2} \right) \tag{11}$$

The complex beam parameter is defined by

$$\frac{1}{q} = \frac{1}{R} - j \frac{\lambda}{\pi w^2} \tag{12}$$

Because $R = \infty$ at the beam waist, the complex beam parameter there is

$$q_0 = j \frac{\pi w_0^2}{\lambda} \tag{13}$$

The complex beam parameter varies along the beam propagation and can be changed by focusing the beam with a thin lens. The complex beam parameter, after propagating a distance d, changes to

$$q' = q + d \tag{14}$$

After the lens, it changes to a new value given by

$$\frac{1}{q'} = \frac{1}{q} - \frac{1}{f} \tag{15}$$

where f denotes the focal length of the lens.

3.2. *Elliptical mirror*

An elliptical mirror can be treated as a simple focusing element with an equivalent focal length f given by

$$\frac{1}{f} = \frac{1}{d_1} + \frac{1}{d_2} \tag{16}$$

where d_1 and d_2 are respectively the distance between focal points and the centre of the cut section of the elliptical surface (figure 4). Although its shape is determined by the incidence angle θ and distances d_1 and d_2, its function is determined only by the focal length f. This result is tested numerically in §4.

3.3. *Application of the complex beam parameter*

As an illustration of the model, we will design a quasi-optical transmission line (see figure 5) to produce a well collimated beam with a waist size of $w_0' = 5.0$ mm.

We first calculate the complex beam parameter q_0 at the image source, using (13) with $w_0 = 25.4$ mm. Next we calculate q at the elliptical mirror, located at a distance d further away, using (14). Next we calculate q' after reflection by the elliptical mirror of focal length f, using (15). We have two parameters that we can adjust,
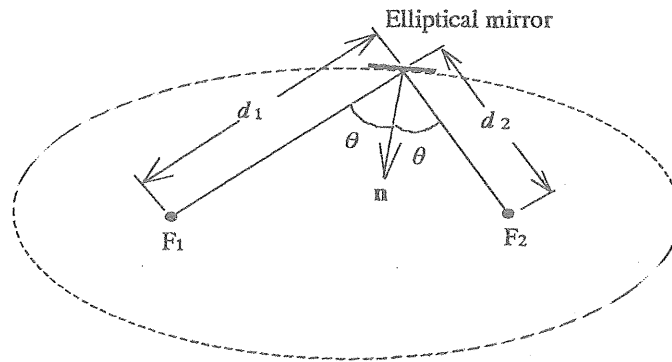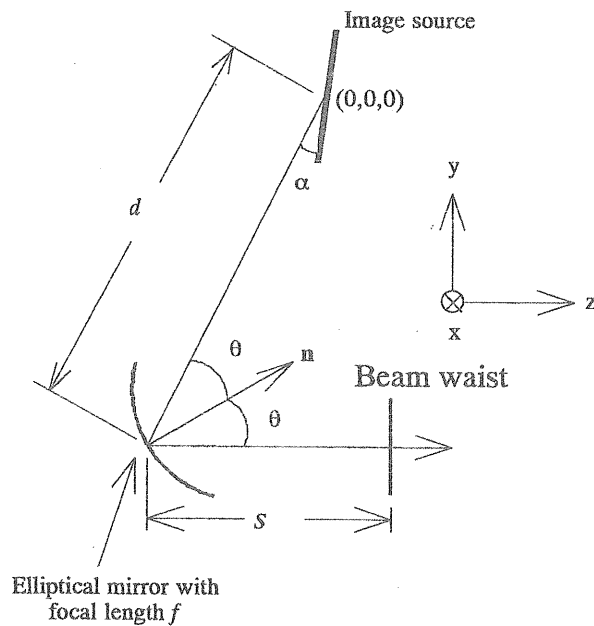
Figure 4. Geometry of elliptical mirror.

Figure 5. Quasi-optical transmission line.

namely d and f, in order to give the desired beam waist $w_0' = 5.0\,\text{mm}$ at the required position $s = 1453\,\text{mm}$. In this case $d = 7000\,\text{mm}$, $f = 1230\,\text{mm}$.

4. Verification of the concept of focal length to wave optics

It is important to see to what extent the reflected beam is influenced by the incident angle θ and the distances d_1, d_2 (see figure 4). Calculations using the Huygens equation have been carried out for $f = 1230\,\text{mm}$ and a mirror of length $W_h/\cos\theta$ and width 240 mm. This mirror projects a rectangle of height W_h and width 240 mm on the x–y plane (figure 5). The dependence of the incident angle is shown in figure 6 and the dependence on the combination of d_1 and d_2 is shown in figure 7. These results prove that incident angle and the combination have little effect on the beams, and support the use of the concept of focal length in wave optics.
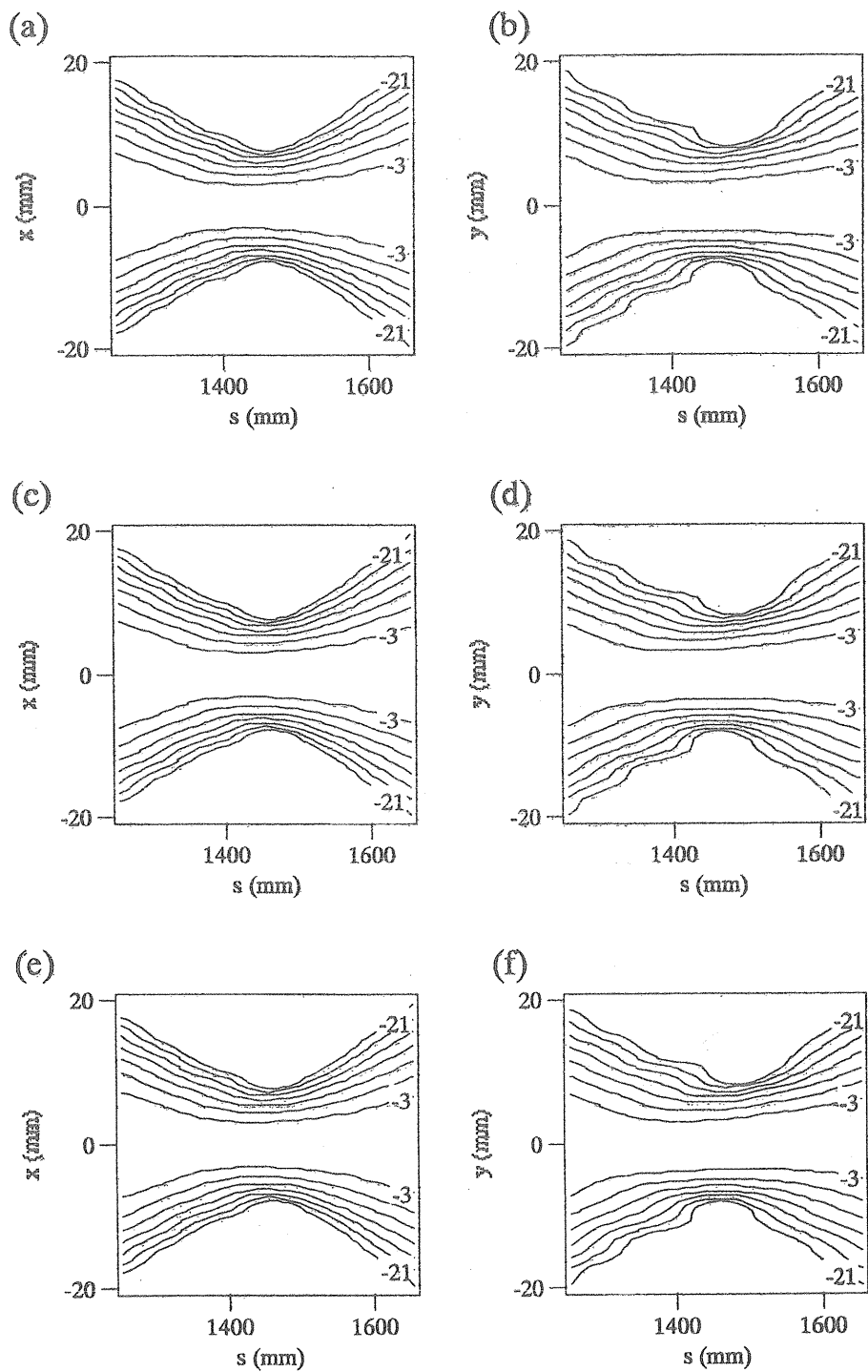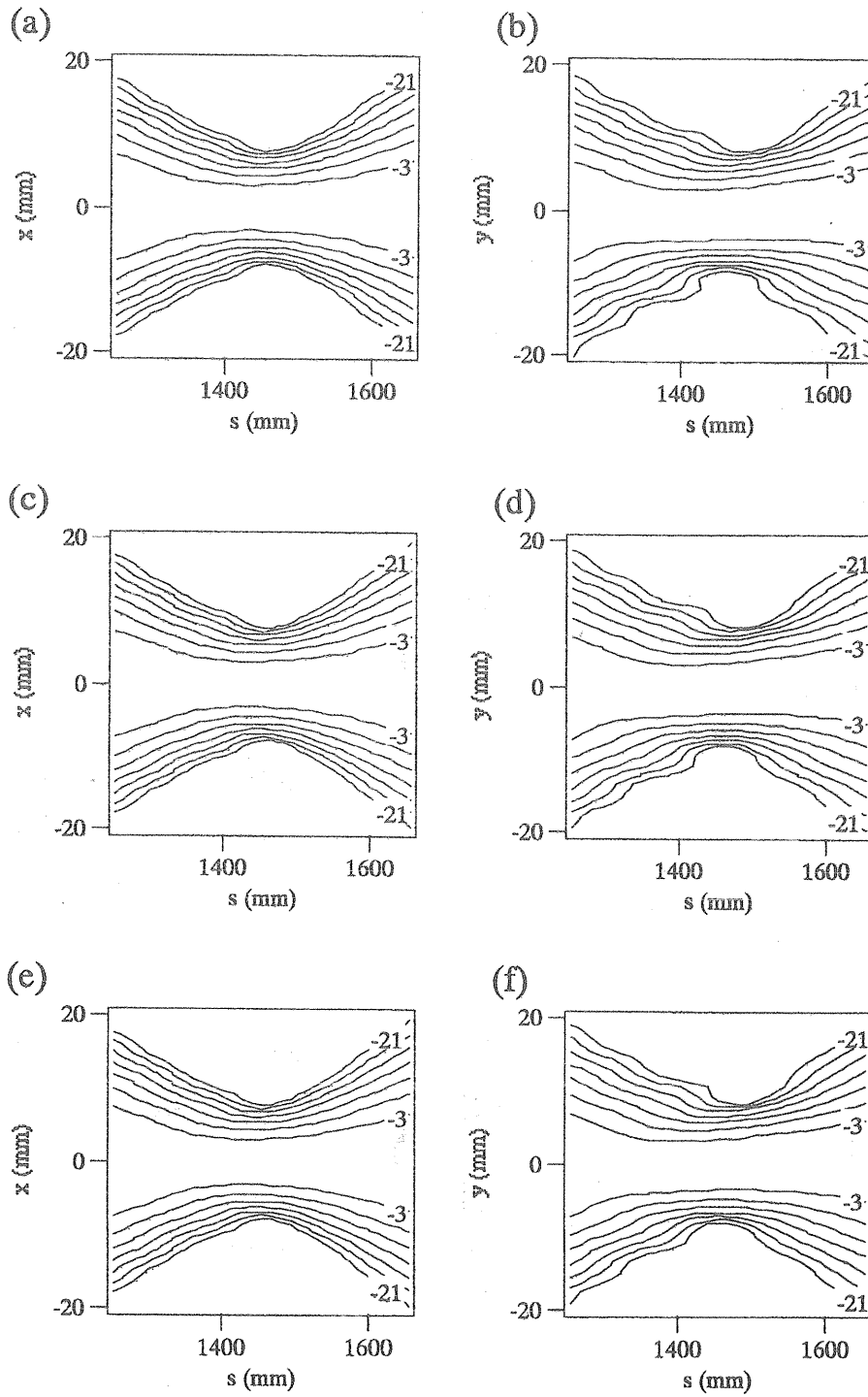
Figure 6. Calculated intensity contours in the x–s plane and the y–s plane. Contours are relative to the intensity along the s-axis. Calculations are carried out under the conditions of $d_1 = 7000$ mm, $d_2 = 1492$ mm and $W_h = 210$ mm. (*a*), (*b*) $\theta = 0°$; (*c*), (*d*) $\theta = 22.5°$; (*e*), (*f*) $\theta = 45°$.

Figure 7. Calculated intensity contours in the x–s plane and the y–s plane. Contours are relative to the intensity along the s-axis. Calculations are carried out for $\theta = 45°$ and $W_h = 210$ mm. (a), (b) $d_1 = 5000$ mm, $d_2 = 1631$ mm; (c), (d) $d_1 = 7000$, $d_2 = 1492$ mm; (e), (f) $d_1 = 10\,000$ mm, $d_2 = 1402$ mm.

5. Influence of the elliptical mirror size on the beam shape

The beam produced by the image source contains sidelobes in addition to the main beam, as can be seen in figure 3(c). The quality of the beam is improved by truncating the sidelobes, which is done by limiting the size of the elliptical mirror. Calculated intensity contours at the beam waist for different mirror sizes W_h are shown in figure 8. A wider mirror distorts the beam because there are contributions from the sidelobes (figure 8(c) and (d)). On the other hand, a smaller mirror truncates the main beam and produces an elongated beam (figure 8(a)). The optimum mirror size which truncates the sidelobes but does not add any distortion of its own is shown in figure 8(b). In spite of the truncation of the sidelobes, most of the power from the image source (89.3%) is still reflected by the mirror.
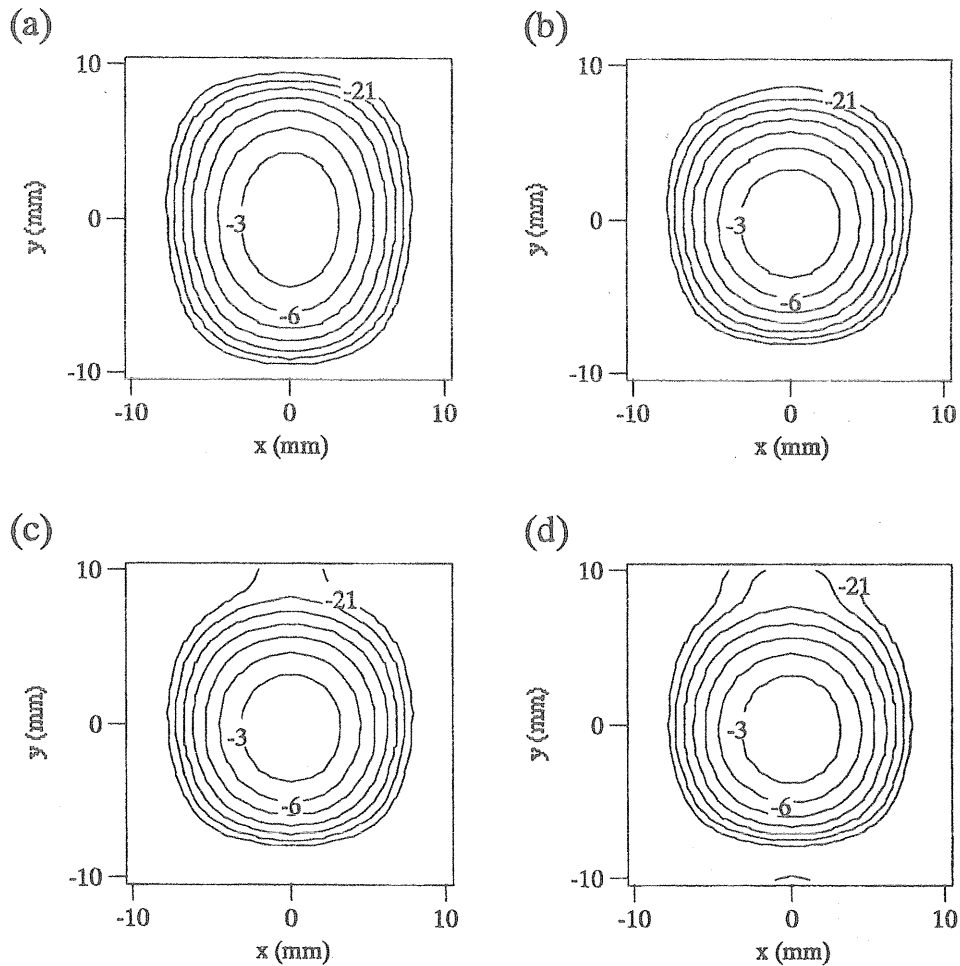
Figure 8. Calculated intensity contours at the beam waist predicted by the beam parameter ($s = 1453$ mm). Calculations are carried out for $d_1 = 7000$ mm, $d_2 = 1492$ mm, $\theta = 45°$. (a) $W_h = 141$ mm; (b) $W_h = 210$ mm; (c) $W_h = 248$ m; (d) $W_h = 283$ mm.

6. Verification of estimation by the complex beam parameter

The complex beam parameter has been applied to the design of systems, producing beams with different waist sizes of $w_0' = 2.0$ mm, 10.0 mm and 15.0 mm as well as $w_0' = 5.0$ mm. Calculated intensity contours are shown in figure 9. The corresponding
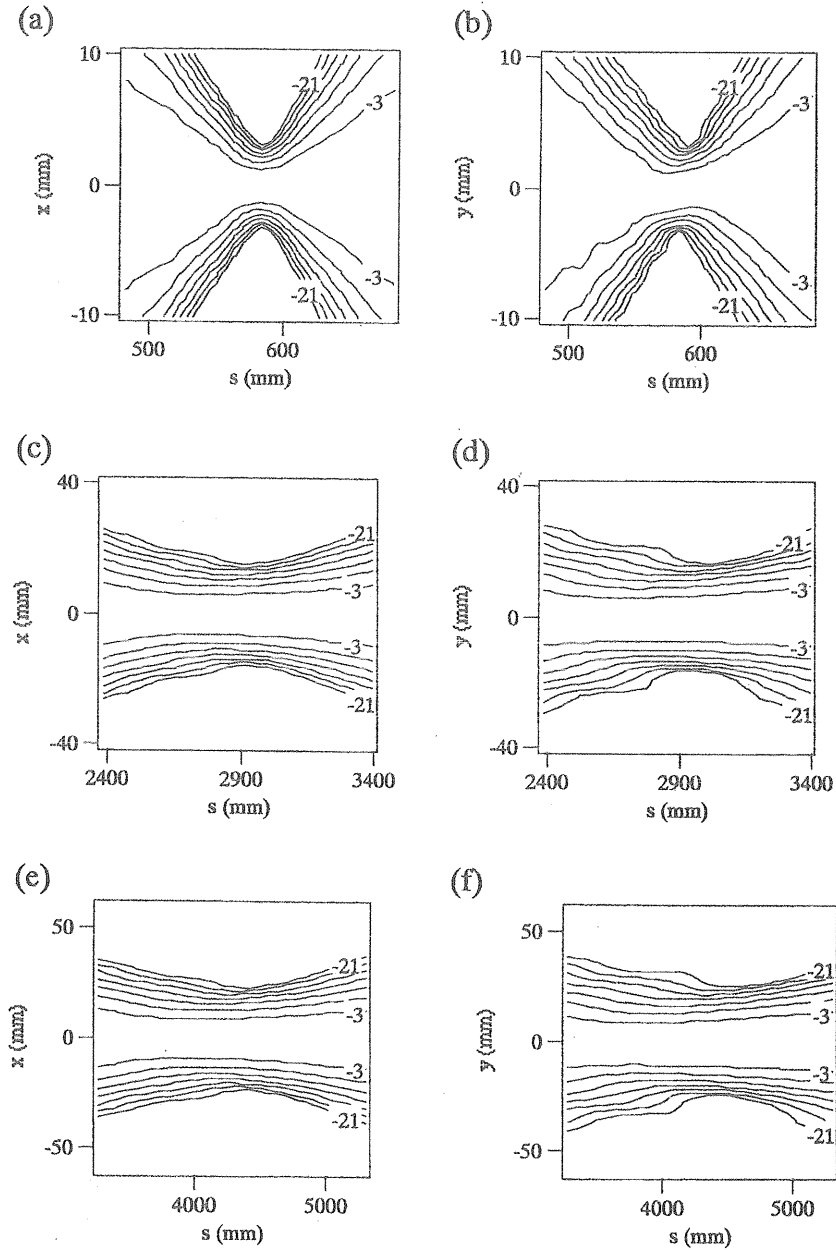

Figure 9. Calculated intensity contours in the x–s plane and the y–s plane. Contours are relative to the intensity along the s-axis. Calculations are carried out for $\theta = 45°$, $W_h = 210$ mm and $d_1 = 7000$ mm. (a), (b) $w_0' = 2.0$ mm, $d_2 = 588$ mm; (c), (d) $w_0' = 10.0$ mm, $d_2 = 3071$ mm; (e), (f) $w_0' = 15.0$ mm, $d_2 = 4767$ mm. w_0' denotes the objective waist size.

focal lengths f and the distances s from the elliptical mirror to the beam waist (see figure 5) are listed in table 3. The waist sizes w'_{0x} and w'_{0y} and its distances s_x and s_y obtained by a Huygens equation calculation are also listed in table 3, for comparison. The results obtained by the complex beam parameter approach are in good agreement with the calculations. Calculated intensity contours at the beam waist predicted by the complex beam parameter are shown in figure 10.

w'_0 (mm)	f (mm)	s (mm)	w'_{0x} (mm)	s_x (mm)	w'_{0y} (mm)	s_y (mm)
2.0	542	582	2.1	583	2.3	584
5.0	1230	1453	5.3	1450	5.7	1450
10.0	2134	2889	10.6	2828	11.4	2811
15.0	2836	4288	15.5	4143	17.0	4049

Table 3. Waist sizes w'_0 and distances s from the elliptical mirror to the beam waist. The value of w'_0 is a target waist size of the beam produced. That of f denotes the focal length determined by the complex beam parameter. The values of w'_{0x} and w'_{0y} are waist sizes obtained by calculations.
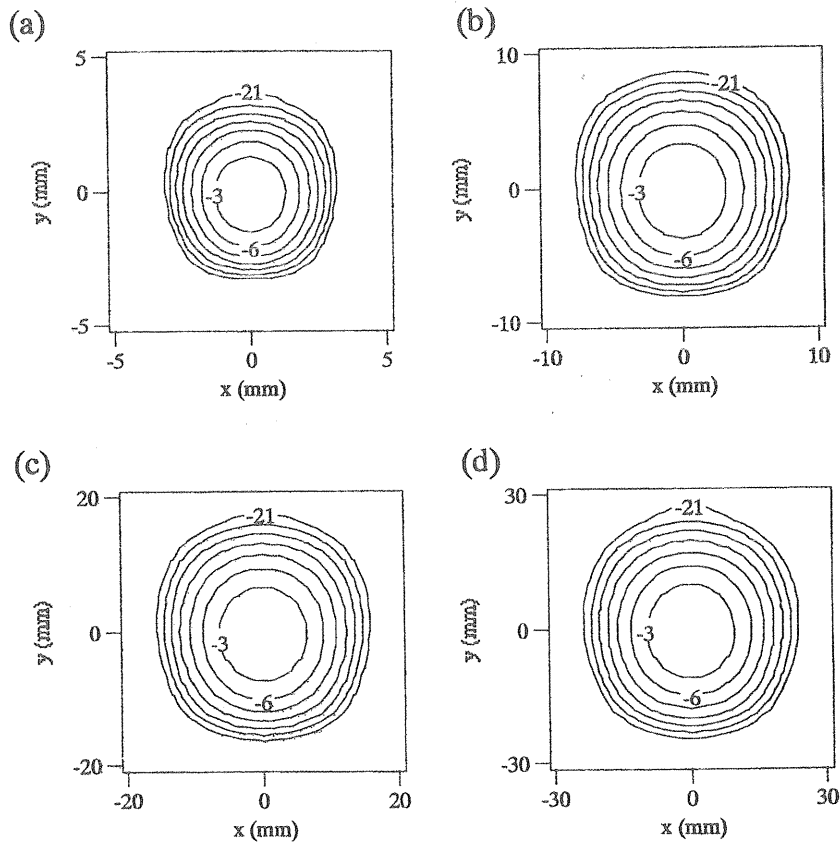

Figure 10. Calculated intensity contours at the beam waist predicted by the beam parameter. Calculations are carried out for $\theta = 45°$, $W_h = 210$ mm and $d_1 = 7000$ mm. (a) $w'_0 = 2.0$ mm, $d_2 = 588$ mm, $s = 482$ mm; (b) $w'_0 = 5.0$ mm, $d_2 = 1492$ mm, $s = 1453$ mm; (c) $w'_0 = 10.0$ mm, $d_2 = 3071$ mm, $s = 2889$ mm; (d) $w'_0 = 15.0$ mm, $d_2 = 4767$ mm, $s = 4288$ mm. w'_0 denotes the objective waist size.

7. Conclusion

The quasi-optical transmission line described here is able to convert the gyrotron output into a well collimated, linearly polarized beam. For the sake of beam quality, non-paraxial components and sidelobes of the beam produced by the quasi-optical antenna are removed by locating an elliptical mirror of suitable size far from the antenna. Very little ($< 11\%$) of the beam power is lost.

Calculations using the Huygens equation confirm that the propagation of the beam produced by the image source can be treated by Gaussian optics far from the source and that the usual geometrical optics concept of focal length is useful here. This allows us to apply the complex beam parameter to the design of transmission lines to produce beams with the spot size we require. Using this approach requires much less computation time.

References

BRAND, G. F., FEKETE, P. W., IDEHARA, T., and MOORE, K. J., 1990, Quasi-optical antennas for plasma scattering. *International Journal of Electronics*, 68, 1063–1073.

FEKETE, P. W., BRAND, G. F., and IDEHARA, T., 1994, Scattering from discrete Alfven waves in a tokamak using a gyrotron radiation source. *Plasma Physics and Controlled Nuclear Fusion*, 36, 1407–1417.

HONG, K. D., BRAND, G. F., FEKETE, P. W., and IDEHARA, T., 1992, Submillimeter wave generation by second harmonic operation of tunable gyrotrons. *International Journal of Infrared and Millimeter Waves*, 13, 215–227.

IDEHARA, T., TATSUKAWA, T., OGAWA, I., TANABE, H., MORI, T., WADA, S., BRAND, G. F., and BRENNAN, M. H., 1992, Development of a second cyclotron harmonic gyrotron operating at submillimeter wavelengths. *Physics of Fluids*, B4, 267–273.

IDEHARA, T., TATSUKAWA, T., OGAWA, I., SHIMIZU, Y., MAKINO, S., and KANEMAKI, T., 1993, Development of a high-frequency, second-harmonic gyrotron tunable up to 636 GHz. *Physics of Fluids*, B5, 1377–1379.

KAWAHATA, K., TETSUKA, T., FUJITA, J., NAGATSU, M., OHNISHI, H., OKAJIMA, S., and IWEASAKI, T., 1988, HCN laser scattering on the JIPP T-IIU tokamak. *International Journal of Infrared and Millimeter Waves*, 9, 655–665.

OGAWA, I., SAKAI, A., IDEHARA, T., KAWAHATA, K., and KASPAREK, W., 1997, A quasi-optical transmission line for plasma scattering measurements using a submillimeter wave gyrotron. *International Journal of Electronics*, 83, 635–644.

SEMET, A., MASE, A., PEEBLES, W. A., LUHMANN, N. C., ZWEBEN, S., Jr, 1980, Study of low-frequency microturbulence in the Microtor tokamak by far-infrared laser scattering. *Physical Review Letters*, 45, 445–448.

SUVOROV, E. V., HOLZHAUER, E., KASPAREK, W., LUBYAKO, L. V., BUROV, A. B., DRYAGIN, Y. A., FIL'CHENKOV, S. E., FRAIMAN, A. A., KUKIN, L. M., KOSTROV, A. V., RYNDYK, D. A., SHTANYUK, A. M., SKALYGA, N. K., SMOLYAKOVA, O. B., ERCKMANN, V., GEIST, T., KICK, M., LAQUA, H., and RUST, M., 1997, Collective Thomson scattering at WA-AS. *Plasma Physics and Controlled Fusion,* **39,** B337–B351.

VLASOV, S. N., and ORLOVA, I. M., 1974, Quasioptical transformer which transforms the waves in a waveguide having a circular cross section into a highly directional wave beam. *Radiofizika,* **17,** 115–119.

WADA, O., and NAKAJIMA, M., 1986, Reflector antennas for electron cyclotron resonance heating of fusion plasma. *Space Power,* **6,** 213–220.